International Journal of Marine Engineering Innovation and Research, Vol. 10(3), Sept. 2025. 1041-1054
(pISSN: 2541-5972, eISSN: 2548-1479)

A Direct Measurement of Vibration on the HDPE Structure of POLBENG Research Boat

Muhammad Alimul Hafiz[1], Muhammad Sidik Purwoko [2*], Fazrian [3], Rizky Chandra Ariesta [4], Jamal [5], Arief Teguh Pribadi [6], Diki Arnanda[7], Mhd Vikri Ardiyanto[8], M Ibrahim Anselistyo[9]

(Received: 22 August 2025 / Revised: 29 August 2025 /Accepted: 7 September 2025 / Available Online: 30 September 2025)

***Abstract*— The adoption of High Density Polyethylene (HDPE) as the primary material for boat structures has increased significantly in recent years. In response to contemporary challenges and to facilitate research requirements, Polytechnic of Bengkalis (POLBENG) constructed a research boat utilizing HDPE. Nevertheless, further research on the response of the HDPE structure to vibrations generated by the main propulsion engine remains insufficiently intensive. Therefore, a direct measurement of ship vibration is conducted utilizing vibration sensors, namely Witmotion WTVB02-485. Both inside and outside of the accommodation rooms, measurements were taken. By comparing the vibrational velocity's Root Mean Square (RMS) to standards established by the American Bureau of Shipping (ABS), a classification society, structural assessment was evaluated. Furthermore, resonance events were discovered by comparing the Blade Passing Frequency (BPF) with the recorded peak frequency output. The HDPE structure seems to be dependable, according to the measurement findings at both locations. The RMS of 0.020 mm/s and a peak frequency of 33.31 Hz were recorded inside the accommodation area, whereas 0.013 mm/s and 31.52 Hz were recorded outside.**

Keywords—high density polyethylene; vibrations; direct measurement.

[*]*Corresponding Author:mhafiz@polbeng.ac.id*

I. INTRODUCTION

The extensive application of HDPE (High Density Polyethylene) in maritime structures commenced in the 2000s. At that time, it was utilized solely as a support structure, rather than as the primary structural material. HDPE is a linear thermoplastic polymer derived from ethylene monomer [1]. The density of HDPE is between 946 and 972 kg/m³ [2], which is less than that of water. The material exhibits an average yield stress of 18.34 MPa, an ultimate stress of 24.73 MPa, and an elongation of 228.36%, as determined from tensile tests conducted on seven samples [3]. This material became popular over time due to its remarkable strength, elevated stiffness, resilience to environmental conditions, and improved thermal resistance compared to other polymers like Low Density Polyethylene (LDPE) and Linear Low Density Polyethylene (LLDPE) [4], [5], [6], [7], [8]. In addition to its advantage, HDPE is recognized for its recyclability, enhancing its economic value, lightweight properties, environmental sustainability, the ability to endure high impact loads, possesses significant tensile strength, can tolerate continuous weather changes, and exhibits resistance to scratches, dirt, and corrosion [9], [10], [11], [12], [13]. Modern materials must exhibit enhanced eco-friendly properties, as plastic has been integral to human life for over 60 years, resulting in numerous detrimental effects on the environment [1]. Approximately 140 million tons of plastic waste contaminate the oceans [14], [15]. Consequently, HDPE emerged as the primary material for ship structures, particularly in small vessels, during the early 2010s. The properties of this material are well-suited for ship operational conditions, leading to its widespread use in the construction of small vessels, including patrol boats, fast boats, rescue boats, and lifeboats [16]. As a relatively novel material for ship structures, comprehensive studies are essential to examine the impacts of various loads, including vibration, on these boat structures.

The current discourse on this material encompasses various themes, including the experimental comparison of tensile tests between virgin HDPE and recycled HDPE [17], the examination of bending durability in composite materials made from HDPE waste and wood waste [18], and the examination of how the composition of LDPE and HDPE mixtures influences their mechanical properties [19]. In the field of naval architecture, various research themes have emerged, including finite element analysis (FEA) of 38-foot ships constructed from HDPE

Muhammad Alimul Hafiz, Department of Naval Architecture, Polytechnic of Bengkalis, Bengkalis, 28711, Indonesia. E-mail: mhafiz@polbeng.ac.id
Muhammad Sidik Purwoko, Department of Naval Architecture, Polytechnic of Bengkalis, Bengkalis, 28711, Indonesia. E-mail: m.sidikpurwoko@polbeng.ac.id
Fazrian, Department of Naval Architecture, Polytechnic of Bengkalis, Bengkalis, 28711, Indonesia. E-mail: fazrian@polbeng.ac.id
Rizky Chandra Ariesta, Department of Naval Architecture, Technology Institute of Sepuluh Nopember, Surabaya, 60111, Indonesia. E-mail: chandra@its.ac.id
Jamal, Department of Naval Architecture, Polytechnic of Bengkalis, Bengkalis, 28711, Indonesia. E-mail: jamal@polbeng.ac.id
Arief Teguh Pribadi, Department of Naval Architecture, Polytechnic of Bengkalis, Bengkalis, 28711, Indonesia. E-mail: arief@polbeng.ac.id
Diki Arnanda, Department of Naval Architecture, Polytechnic of Bengkalis, Bengkalis, 28711, Indonesia. E-mail: dikiarnanda6@gmail.com
Mhd Vikri Ardiyanto, Department of Naval Architecture, Polytechnic of Bengkalis, Bengkalis, 28711, Indonesia. E-mail: ardiyantovikri@gmail.com
M Ibrahim Anselistyo, Department of Naval Architecture, Polytechnic of Bengkalis, Bengkalis, 28711, Indonesia. E-mail: ibrahimtyo2020@gmail.com

under design loads established by ISO and different classification societies [20], feasibility assessments of welding outcomes on HDPE ship structures [21], and investigations into the design and production of structural components for HDPE ships [11]. At this point, comprehensive research regarding the impact of ship main engine vibration on HDPE ship structures remains scarce. This research gap prompted the initiation of this study.

Vibration refers to the oscillatory motion of an object or its surface relative to its equilibrium position, which is defined as the state of the object at rest and unaffected by external forces [22]. The maximum displacement from the equilibrium position is termed the amplitude. Frequency refers to the number of deviations occurring within a specified time frame. Frequency is categorized into two types: excitation frequency and natural frequency. Excitation frequency refers to the frequency influenced by the excitation load. On ships, excitation can ensue from the operation of the main engine, propellers, auxiliary engines, and wave behaviors [23]. The natural frequency refers to the frequency at which a system undergoes free vibration in the absence of damping. It is a characteristic inherent to all objects possessing mass and stiffness [24].

On average, each ship in the global fleet sustains hull damage once every decade due to hull-side deformation, which is responsible for 53% of maritime accidents [25]. A method for identifying damage is necessary to prevent this, such as utilizing a vibration approach as the observed response parameter. This method has been applied in case studies involving composite materials [26] and cantilever beams [27] for the purpose of detecting structural damage. The analysis method employed to mitigate such damage is modal analysis, which identifies the vibration characteristics of the object, allowing for a comparison of the structure's performance in both damaged and undamaged states [28]. Structural assessment due to vibration is often preceded by damage from resonance phenomena, where the excitation frequency matches the structure's natural frequency [22]. The occurrence of these phenomena lead to an increase in vibration amplitude, subsequently raising dynamic stress levels. Prolonged exposure may result in fatigue [29]. The subsequent domino effect involves the emergence of cracks, which propagate until the structure experiences fracture or failure [30]. This overview emphasizes the need of evaluating the impact of vibration frequency on ship constructions. The American Bureau of Shipping (ABS), a classification society, has set acceptable vibration norms for ship structures. In the frequency range of up to 5 Hz, the permissible displacement is less than 1 mm, while displacements over 2 mm may cause structural damage. In the frequency band above 5 Hz, the permissible vibration velocity is under 30 mm/s, with a potential for structural damage if the velocity exceeds 60 mm/s [23].

Preventing potential damage requires the initial identification of vibrations within the structure. Measurements are required to ascertain the excitation frequency and natural frequency of the structure, followed by engineering resonance to reduce the likelihood of its occurrence. One of the actions taken is to decrease the amplitude of the excitation load from the source, contingent upon the excitation frequency. As an illustration, if a propeller's operation results in excessive vibration, the design can be reexamined. The remedy may involve altering the propeller's diameter, number of leaves, or unsteady propeller hydrodynamics [23]. In the case of the main engine, altering the engine's operating RPM (Revolutions Per Minute) is the countermeasure. The other action to enhance the ship's structural system involves increasing the structure's stiffness, which is commonly applied rather than addressing the excitation load source [23].

This study identifies the ship's main engine as the source of the observed vibration excitation using an experimental method, which is a direct measurement. Experimentation is a research method that entails the direct observation of the dependent variable while regulating the independent variable [31]. The independent variables assessed are the Revolutions Per Minute (RPM) number of the main engine and the measurement location, whereas the dependent variable is the amplitude and frequency of the measured vibration. This method was chosen for its capacity to precisely characterize field conditions.

The WitMotion WTVB02-485 accelerometer sensor is the brand that is utilized for the direct measurement. The sensor provides outputs for displacement, velocity, and linear acceleration across three axes, which can be expressed as functions of time and frequency. The brand has shown it can be worthy trusted, as its sensors have been used in different studies, like measuring vibrations on a pendulum-flywheel [32], a pump engine [33], and in marine uses with a buoy [34], [35]. The direct measurement approach has been employed in various studies utilizing diverse types and brands of sensors, including pressure sensors [36], [37], tactile sensors [38], and different brands of accelerometer sensors [39].

A modal analysis method is employed in the assessment stage, which identifies various modal parameters, including resonant frequency, damping factor, and mode shape [40]. The reason this method was selected is due to its widespread application in structural damage detection, characterized by its ease of implementation and efficiency in terms of time required. This method has been extensively utilized, including in the assessment of damage to bridge structures [41]. It has found extensive use in marine engineering, particularly in model ship testing (direct measurement) [42] and numerical analyses [43].

This study applies modal analysis within an experimental framework. Thus, it is accurately referred to as Experimental Modal Analysis (EMA). As a consequence, there are several assumptions that are applied in this research, such as:

1) The structures are linear, indicating that mass and stiffness remain constant.
2) Damping is negligible due to its minimal effect.
3) Time variation does not influence the structure concerning load, displacement, pressure, and

temperature.

The other research has utilized the EMA approach, such as the research on the ships with the lengths of 212 m and 223 m [44] and the research on the Scottish trawler [45].

This study encompassed the direct measurement of vibrations in HDPE ship constructions, considering the vibrations of the main engine as an excitation load. Measurements conducted within the accommodation room of POLBENG's research vessel using WitMotion WTVB02-485 accelerometer sensor. The objective of the measurement is to determine the excitation frequency being assessed. The natural frequency of the HDPE ship structure is computed to aid in the structural evaluation phase. It employs a modal analysis method that assesses both frequencies. Structural design optimization can be attained by altering the stiffness of the structure. To advance ongoing research, this theme could be incorporated into numerical simulation studies in the next research.

II. Experimental Setup

A. Boat Description

The boat under examination in this study is the POLBENG 1 research boat, owned by Polytechnic of Bengkalis (POLBENG), constructed from High Density Polyethylene (HDPE), and classified as a small ship. **Table 1** presents the boat's main dimensions, while **Figure 1** depicts the ship's documentation. This 9-meter boat is powered by a single 85-hp outboard engine. The boat was constructed and finalized in the year 2024. In the year, the Department of Naval Architecture, in collaboration with the Ministry of Education and Science and CV Fatih Bahari Engineering, received funding from the Matching Fund Research to construct this ship prototype. This prototype is explicitly engineered to facilitate student research and practicum endeavors in marine technology, along with investigations pertaining to coastal waters. The POLBENG 1 research boat is designed to be a teaching tool and a testing site for improving ship technology using eco-friendly, lightweight, and corrosion-resistant HDPE instead of regular materials like steel or wood. The research boat is anticipated to enhance the quality of vocational education and fortify the collaboration between universities and industry in advancing maritime technology in Indonesia.

Table 1
Research Boat Main Dimensions

Parameter	Dimensions
Length Overall	9 m
Length Perpendicular	8.94 m
Breadth	2.2 m
Depth	1.2 m
Designed Draught	0.45 m
Service Speed	15 knot
Block Coefficient	0.479

Figure 1. POLBENG research boat.

B. Experimental Equipment

The equipment utilized in the study was categorized into two types: hardware and software. Both were utilized to facilitate the testing stage until the data processing stage. The hardware utilized are as follows:

1) The vibration sensor employed in this study is the WTVB02-485, produced by WitMotion Shenzhen Co. Ltd. This sensor is compact, with dimensions of 47 mm x 38 mm. The **Figure 2** depicts the employed sensor. The detection cycle, denoting the quantity of data points produced per second, can be adjusted between 1 and 200 Hz. The sensor exhibits an accuracy level with a data error rate of approximately 4% of the total data during measurement. If the measurement produces 15,000 data points, the data error would consist of 600 data. This sensor quantifies vibrations across three axes. The output data includes acceleration measured in gravity units, velocity in millimeters per second units, and displacement in micrometers units.
2) An ASUSTeK Computer Inc. laptop was utilized for the testing and data processing stages. The laptop model was ASUS ROG GL502VM, featuring an i7 processor and an NVIDIA GeForce GTX 1060 graphics card. During the testing stage, the laptop was utilized to operate software for measuring vibrations. Concurrently, in the data processing stage, the laptop operates data processing software.
3) The Yamaha 85AETX serves as the propulsion engine for the research boat. The engine operates within a maximum range of 4,500 to 5,500 Revolutions Per Minute (RPM), producing 85 horsepower and possessing a cylinder volume of 1140 cc. The engine has a mass of 124 kg and a fuel consumption rate of 35 liter per hours at 5,000 RPM.
4) The main engine's rotation is measured with a digital tachometer featuring a photosensor, namely the DT-6236B model. The **Figure 3** displays the sensor. It can measure RPM ranging from 2.5 to 99,999. The sample time is 0.5 seconds.
5) An anemometer measures wind speed during measurement. The recorded wind speed is expected to be low. The instrument is branded as Benetech GM816. It measures wind speed from 0 to 30 m/s with an accuracy of 5%. This instrument not only measures wind speed but also measures room temperature. It is to facilitate the monitoring of the temperature affecting the HDPE construction. The **Figure 4**

Figure 2. Vibration sensor.

Figure 3. Tachometer.

Figure 4. Anemometer.

depicts the wind speed instrument.

6) A thermogun is employed to measure the water temperature surrounding the hull during the measurement process. It is to facilitate the monitoring of the temperature exposure of the HDPE construction. The instrument's brand is GM320. This instrument may measure temperatures from -50°C to 380°C. This instrument measures temperature using an infrared sensor with the accuracy of 1.5%. **Figure 5** depicts the temperature instrument documentation.

The software utilized are as follows:

1) WitMotion.exe is a program that controls the WTVB02-485 sensor. WitMotion Shenzhen Co. Ltd. is the manufacturer of this software. The software offers data visualization through various graphical representations, including time domain plots and scatter plots. The output data can be extracted into the file types ".csv".
2) MATLAB.exe is a software program that significantly contributes to data processing. This software emphasizes numerical and mathematical computation with an intuitive interface. It is extensively utilized in signal processing. It can subsequently display data in multiple graphical formats, including both 2D and 3D representations.

C. Observed Measurement Points

The measurement points identified are located inside the accommodation room (point A) and outside the accommodation room (point B). Point A locates precisely 3.8 meters from the After Perpendicular (AP), whereas point B is located exactly 2.6 meters from AP. Both points are located transversely and vertically at the center (0.3 meters from the centerline) and on the main deck (0.5 meters from the baseline). **Figure 6** illustrates the locations of the measurement points. Those measurement points are the vibration sensor locations. Both points were measured concurrently in a single test utilizing two sensors of identical type (WTVB02-485). Points A and B are considered equivalent, with the engine RPM measured at full service RPM (4,000 RPM) and a load of 6 individuals. **Figure 6** illustrates the

Figure 5. Thermogun.

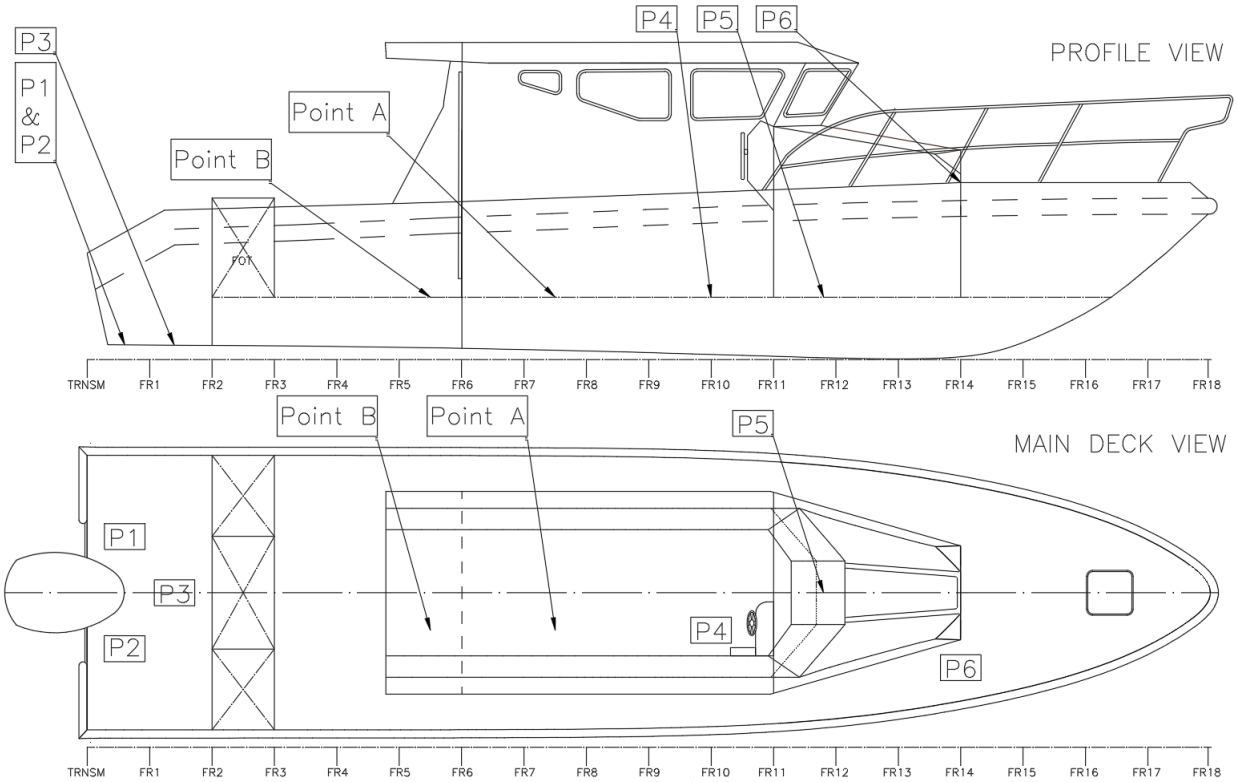

Figure 6. Arrangement drawing.

location of the loaded individuals. Their weights are P1 at 69 kg, P2 at 85 kg, P3 at 42 kg, P4 at 122 kg, P5 at 83 kg, and P6 at 77 kg. There are two measurement cases, both exhibiting identical variations, characterized by fluctuations in RPM of about 4,000 and a total of six individuals. The distinction between the two cases lies in the placement of the vibration sensor; Measurement 1 places the sensor within the accommodation room (Point A), whereas Measurement 2 places it outdoors (Point B).

D. Testing Procedures

The following are the stages in testing procedures:

1) Beginning the process of preparing the experimental equipment. Prepare the boat and the propulsion system in accordance with the requirements. At the appointed measurement points, as shown in **Figure 7**, location the two vibration sensors in the appropriate positions. A laptop should be used to connect the two sensors, and the WitMotion.exe program should be stand by in order to begin the process of measurement. Examine the positions of the individuals to ensure that they are consistent with those shown in **Figure 6.** The tachometer, anemometer, and thermogun are prepared.
2) Initiating the WitMotion.exe program preparation. Select the appropriate sensor model number: WTVB02-485. Verify that the serial port number corresponds to the chosen port. The program is now operational and will present the collected data. Make sure the connection between the laptop and the vibration sensor is not experiencing problems.
3) Observe the initial conditions of the surrounding environment. The environmental conditions that are observed include measurements of the speed of the wind, measurements of the temperature of the water, and observations of wave ripples. The results of the observations are recorded for each individual measurement. **Figure 8** and **Figure 9**

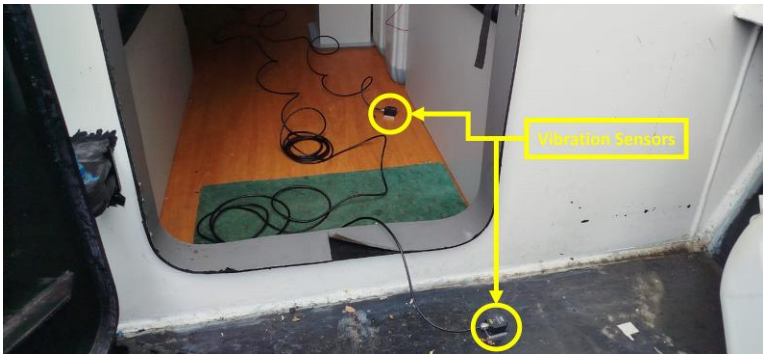

Figure 7. Documentation of the vibration sensor locations.

Figure 8. Measurements of the wind speed.

Figure 9. Measurements of the water temperature.

document the wind speed and water temperature measurements, respectively.

4) Start the engine. Around 4,000 revolutions per minute (RPM) is the required RPM for the main engine to be run at. The RPM number is the operation number at the service speed. This is accomplished by operating the engine in the neutral transmission mode, which prevents the ship from moving in any way. It is important to make sure that the engine is operating consistently at the required RPM while the measurement is conducted. The number is recorded by the tachometer. Its measurement documentation is shown in **Figure 10**.
5) Begin the measurement process. In order to begin the measurement process, select the record button located within the WitMotion.exe program. During the measurement process, check to verify that the WitMotion.exe program is operating correctly. After that, check to ensure that there are no external forces affecting the ship (like wind and waves), and that there are no people moving around.
6) Bring an end to the measurement. As soon as the duration of the data measurement reaches five minutes, the measurement is considered to be finished. The recommendations of the ABS class have been taken into consideration when determining this duration. The program that is currently running should be terminated once this time period has been reached, and then the raw data should be extracted using the Comma Separated Values (.csv) file type.
7) Take note of the final conditions of the environment. It is the same actions that were taken in step 3 that are being taken at this stage. Then, a summary of all the data from the observations is gathered, including both the initial and the final observations.

E. Data Processing

The raw data is presented in the time domain after extraction and depicts the vibration produced by the excitation load. The vibration velocity along the Z-axis (vertical movements) is the raw data recorded by the accelerometer sensor. It requires processing to yield usable data. Data processing comprises two stages: the filtering stage and the transforming stage. All stages are executed using the Matlab.exe software. The first is the filtering stage. A signal dataset invariably contains noise captured during the measurement process. This can be mitigated by employing filtering methods in data processing, specifically through the application of the Moving Average Filter (MAF) method in this study. MAF is a technique for reducing noise in a signal while maintaining its unique characteristics, achieved by averaging successive points of the input signal to produce each point of the output signal [46]. This method has been extensively utilized in engineering, including energy consumption management in cars [47] and ships [48], data processing of monocular cameras on Unmanned Surface Vessels for ship tracking [49], and facilitating direct measurements with magnetometer sensors [50]. **Equation (1)** presents the MAF equation.

$$y(i) = \frac{1}{M}\sum_{j=0}^{M-1} x(i+j) \tag{1}$$

Where $y(i)$ is the output signal, $x(i+j)$ is the input signal, and M is the number of samples.

The process of averaging a signal is fundamentally analogous to the smoothing of that signal or the application of low-pass filtering techniques. The primary benefit of employing MAF lies in the algorithm's straightforwardness, while a significant drawback is the potential loss of information when M is substantially increased [46]. At the optimal value of M, this algorithm preserves the spikes, which represent significant events within the signal. However, if we increase M excessively, the algorithm smooths the signal to such an extent that it may lose crucial data. **Figure 11** illustrates the filtering stages outcomes.

This study proposes the evaluation of structural assessments through frequency domain data to facilitate visual observation. The filtered data must be transformed

from the time domain to the frequency domain. The frequency domain was chosen for its capacity to facilitate visual analysis of a graphic, emphasizing the peak excitation frequency. Subsequently, its peak value is compared to the natural frequency. This study employs the Fast Fourier Transform (FFT) to convert time domain data into frequency domain data, specifically the Power Spectral Density (PSD) estimate. This computation functions as an efficient algorithm for calculating the Discrete Fourier Transform (DFT) of a sequence or its inverse, facilitating the transformation of signals between the time domain and the frequency domain, and vice versa [51]. The Welch method, devised by Peter D. Welch, is one approach for executing this FFT computation. This method is frequently employed in engineering to address signaling issues, including the detection of damage in concrete-filled steel tube columns [52] and the assessment of sea condition parameters by spectral estimation [53]. **Equation (2)** is solved in order to implement this method [54], [55].

$$S_{ZZ}(f) = \frac{2}{n_d N T_S} \sum_{m=1}^{n_d} |Y_m(f)|^2 \tag{2}$$

Where

$$Y_m(f) = T_S \sum_{t=1}^{N-1} w[t]\, y_{k,m}[t]\, e^{-j2\pi f t T_S} \tag{3}$$

and

$$f = \frac{0}{T_S N}, \frac{1}{T_S N}, \frac{2}{T_S N}, \frac{3}{T_S N}, \ldots\ldots \frac{1}{2T_S} \tag{4}$$

In this context, n_d represents the count of overlapping segments, while N denotes the total number of samples, T_S indicates the sampling period, and y_k denotes a particular record at position k. The variable $w[t]$ represents the window function, while j signifies the imaginary unit.

In FFT computations involving real-valued sequences, the results in the frequency domain demonstrate symmetry, which requires the preservation of only half of the outcomes [56]. The results in the frequency domain for FFT computations of complex-valued sequences include both positive and negative frequency components. **Figure 12** illustrates the outcomes of the transforming stages.

F. Natural Frequency Calculation

It is undoubtedly possible for any object with mass and stiffness to have its natural frequency values. The vibration frequency is solely determined by the inherent properties of the system, independent of the initial conditions [57]. Consequently, the subsequent step is to ascertain the natural frequency of the system's observed property, specifically the HDPE ship structure. Numerous methods exist to determine this, including the BPF (Blade Passing Frequency) approach.

Blade Passing Frequency (BPF) refers to the vibration generated by the propeller blades on the ship. This study only examines external excitation forces in the form of propulsion rotation, so the BPF approach is taken into account. Increased frequency generated by the propulsion system can adversely affect its operation, leading to a release of disruptive noise [58], [59], [60]. The resulting frequency may also be considered for the determination of a system's natural frequency. This method has been extensively applied across multiple industrial sectors, including the assessment of comfort levels in centrifugal fans through quantitative study [61],

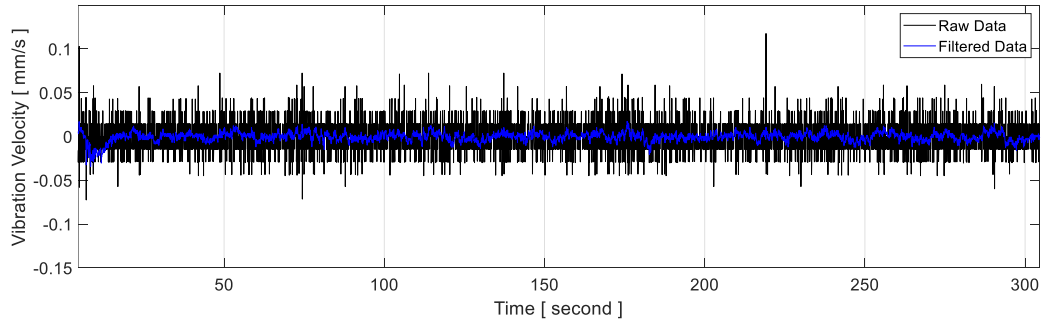

Figure 11. Example of the filtering stage outcome.

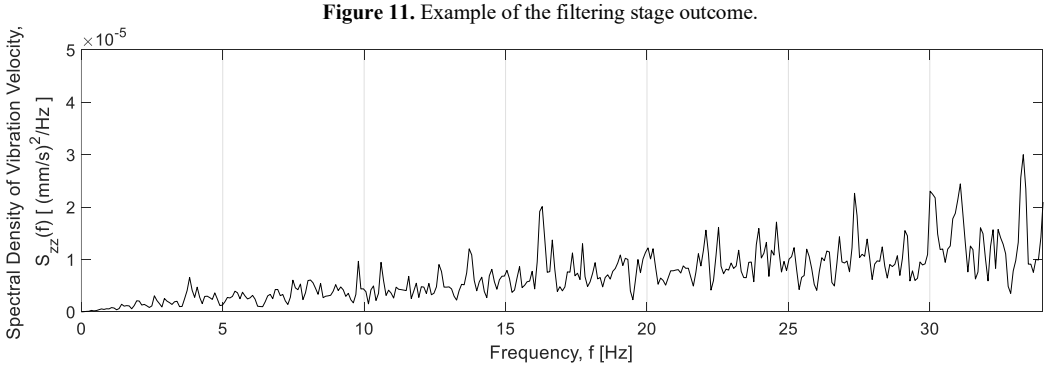

Figure 12. Example of the transforming stage outcome.

the analysis of fault diagnosis models for rotating machinery [62], investigations into BPF pressure pulsation reduction in centrifugal bladed machines utilizing splitters [63], examinations of the impact of blade trajectory frequency vibrations on MCSA-based induction motor rotor fault detection [64], as well as both experimental and numerical studies on flow-induced vibrations and acoustic radiation from a jet-pump propulsor model [65]. While in the domain of naval architecture, topics include the investigation of vibration features in marine propulsion systems [66] and the analysis of fluid-structure interaction concerning rudder vibration in wake propellers [67]. **Equation (5)** shown the BPF formula.

$$BPF = B_n \frac{N_{RPM}}{60} \tag{5}$$

Where B_n is blade number of propeller and N_{RPM} is number of the motor rotating in RPM. The greater the motor's RPM, the higher the BPF. The RPM number (N_{RPM}) is measured by the tachometer.

G. Assessment Procedures

This paper presents a method for evaluating ship structure assessment by comparing the Root Mean Square (RMS) of vibration data from excitation loads with established class standards, such as those set by the American Bureau of Shipping (ABS). **Equation (6)** represents the RMS equation. The comparative excitation data pertains to vibration velocity. In the frequency range up to 5 Hz, the allowable displacement is under 1 mm, as displacements exceeding 2 mm may result in structural damage. For frequencies above 5 Hz, the allowable vibration velocity is below 30 mm/s, with a risk of structural damage if it surpasses 60 mm/s [23].

$$RMS = \sqrt{\frac{1}{M}\left(\sum_{i-1}^{M}\left(x_i - \bar{x}\right)\right)} \tag{6}$$

Additionally, a particular resonance phenomenon is the basis for the other method that is being utilized in this investigation to mitigate the structural failure that is caused by vibration. Failure occurs when the peak frequency of the excitation load coincides with the natural frequency (using the BPF method). An increase in the difference value between the peak excitation frequency and the natural frequency results in a decrease in the chance of resonance and structural failure.

III. Results and Discussion

A direct measurement method has been utilized to measure vibrations in HDPE vessel structures, with the primary source of vibration being the main engine. Vibration is measured via an accelerometer sensor, namely the Witmotion WTVB02-485. The preceding chapter addressed equipment and data processing. Chapter III encompasses a discourse on environmental information obtained through direct measurement, output data articulated in the time domain, processed data delineated in the frequency domain, and evaluation.

A. Recorded Environmental Information

Direct measurements were conducted on August 12, 2025, in the ship launching area of the shipyard at the Shipping Engineering Department, Polytechnic of Bengkalis, as seen in **Figure 1**. The measurement period commences at 10:20 WIB and concludes at 10:26 WIB. During the measurement, it may be assured that no other vessels are transiting, as it is located in enclosed seas. **Table 2** presents the environmental data obtained during the direct measurement.

The air and water temperature measurements presented in **Table 2** indicate consistent values of 29°C and 28°C, respectively. The temperature measurement was conducted to provide information on the temperature at the time of measurement, as it is likely to influence the material properties of the HDPE utilized. This paper will not address details; however, the data presented may be beneficial for future research endeavors.

There were calm waves with very slight ripples during the direct measurement, but no significant wave ripples. The boat's location in enclosed waters may have had an impact on this situation. Alongside visual

Table 2
Summary of recorded environmental information

Time (WIB)	Air Temperature (°C)	Water Temperature (°C)	Wind Velocity (m/s)	Wave Ripples
10.20	31	30	1,1	Very slight ripples
10.21	31	30	1,1	Very slight ripples
10.22	31	30	1,2	Very slight ripples
10.23	31	30	0,8	Very slight ripples
10.24	31	30	0,4	Very slight ripples
10.25	31	30	0	Very slight ripples
10.26	31	30	0	Very slight ripples

observations, measurements of wind speed corroborated this finding. **Table 2** presents the maximum recorded wind speed of 1.2 m/s. This speed remains categorized as Beaufort 1, which the description is that ripples resembling scales are generated, lacking foam crests [68]. The results of these observations and measurements indicate minimal environmental influence on fishing boat vibration measurements. This study advocates for the execution of direct measurements in enclosed waters.

B. Recorded RPM Number

During the direct measurement, the main engine of the ship is capable of operating at optimal levels, adhering to the specified RPM, which is approximately 4,000. **Figure 13** presents the results obtained from measurements conducted with a tachometer. The recorded RPM values ranged from a minimum of 3,702 to a maximum of 4,348. The recorded RPM amounts yield an average of 4,007.3 and a root mean square (RMS) value of 4,011.5.

C. Time Domain Data

The Witmotion WTVB02-485 sensor generates output in the form of raw data representing vibration velocity. The output appears in the time domain. **Figure 14** presents the raw data collected at Point A (Measurement 1), whereas **Figure 15** presents the data from Point B (Measurement 2). The raw data requires processing, specifically during the filtering stage, before it can be assessed directly. The outputs of the filtering stage for Measurement 1 and Measurement 2 are presented in **Figure 16**, respectively. The maximum recorded amplitudes are -0.034 mm/s for Measurement 1 and 0.016 mm/s for Measurement 2. The measurement results within the accommodation room indicate greater amplitude maximum values compared to outside the room.

D. Frequency Domain Data

The filtered data gets transformed from its original representation in the time domain into the frequency domain. The transformation process is referred to as a Power Spectral Density (PSD) estimate. Its computation process is referred to as Fast Fourier Transform (FFT), which is solved using Welch's method. The transforming stage is essential for determining the peak excitation frequency value. Subsequently, a comparison of the peak frequency value is conducted with the natural frequency. Hopefully, the two values will not overlap. **Figure 17**

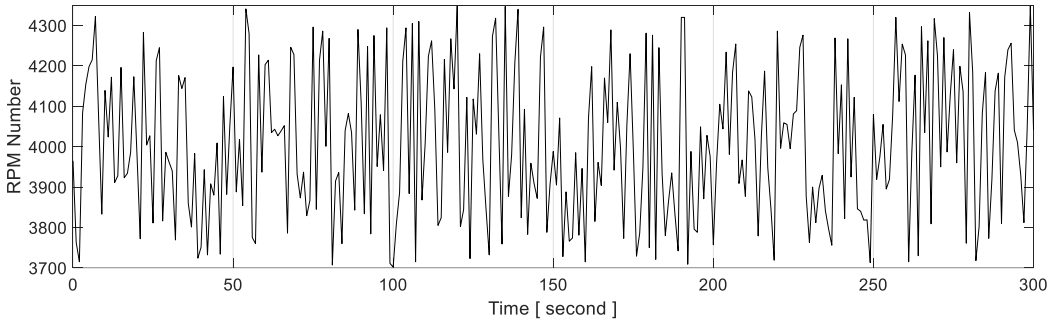

Figure 13. Recorded RPM number.

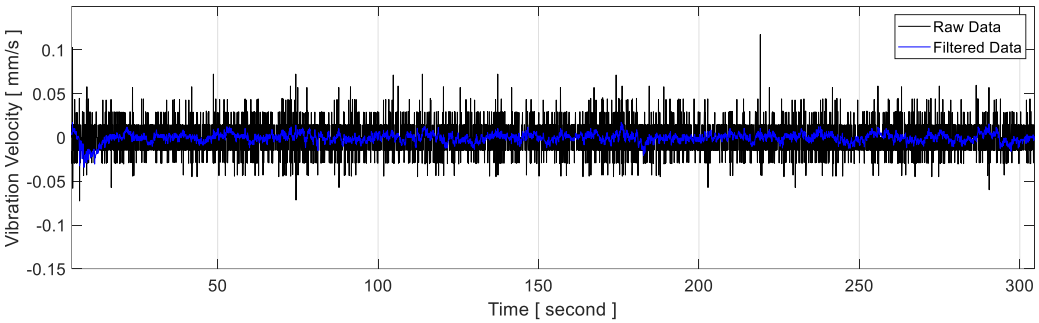

Figure 14. Raw data of Measurement 1 in time domain.

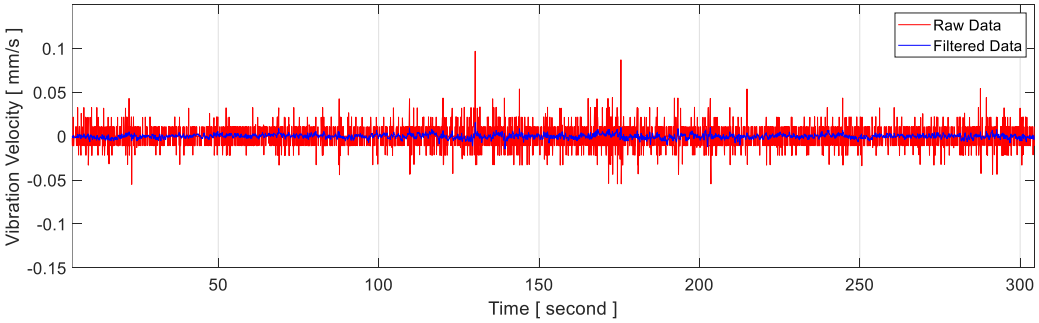

Figure 15. Raw data of Measurement 2 in time domain.

illustrates the outcomes of the transforming stage process for Measurements 1 and 2, respectively. The peak

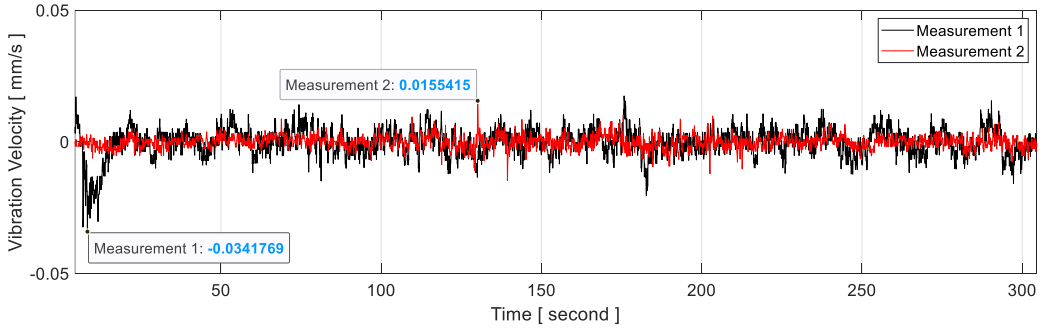

Figure 16. Filtered data of Measurement 1 and 2 in time domain.

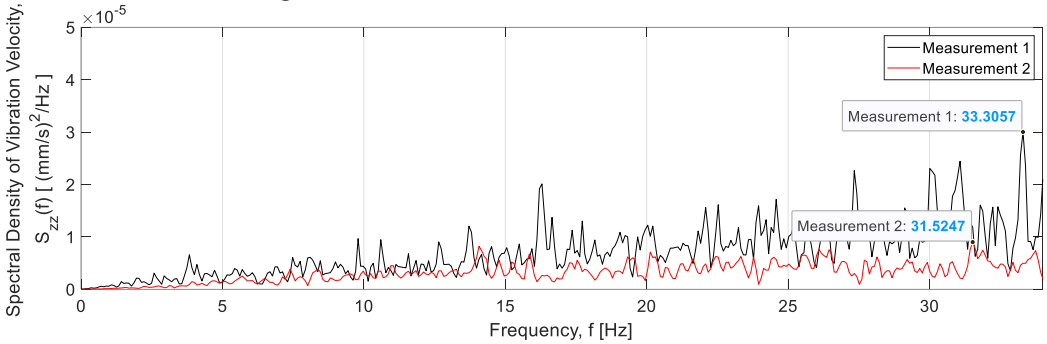

Figure 17. Frequency domain data of Measurement 1 and 2.

frequencies of vibration velocity identified in both figures are 33.31 Hz for Measurement 1 and 31.52 Hz for Measurement 2.

E. Discussion

The average RPM value presented in **Figure 13** is 4,007.3. The integration of this value with **Equation (5)** allows for the calculation of the natural frequency, resulting in a value of 200.4 Hz. Upon comparison of this value with the peak frequency of excitation at both measurement locations, resonance is not discovered. The peak frequency values at the two locations are significantly lower than the natural frequency. The peak frequency recorded in Measurement 1 is 83.34% less than the natural frequency, whereas Measurement 2 is 84.27% less than the natural frequency. Based on this observation, it can be concluded that the HDPE structure is capable of withstanding the vibrations produced by the main engine of the POLBENG research vessel.

According to **Figure 17**, the peak frequency values for Measurement 1 and Measurement 2 are greater than 5 Hz. The RMS values are confirmed to remain below the limit value of 30 mm/s as established by ABS guidelines. The root mean square (RMS) values for Measurement 1 and Measurement 2 are 0.020 mm/s and 0.013 mm/s, respectively. The RMS values for Measurement 1 and Measurement 2 are 99.93% and 99.96% lower than the standard values, respectively. The structural design of the research vessel constructed from HDPE is capable of withstanding vibrations generated by the main engine during operation at RPM of full service speed. It is important to note that the load is exclusively derived from the main engine of the ship. Additional loads, such as those resulting from vibrations caused by the ship's motion due to the interaction between the ship's hull and ocean waves, require further investigation. The research results presented in this paper may be utilized for subsequent experimental development. The results may serve as a reference for structural design development and numerical analysis.

In the process of comparing the output from each observation location. Measurement 1, located within the accommodation room (Point A), exhibits a higher vibration velocity response compared to Measurement 2, which is located outside the room (Point B). The RMS value in Measurement 1 exceeds that of Measurement 2 by 53.85%. The peak frequency value in Measurement 1 exceeds that of Measurement 2 by 5.37%. The occurrence of both phenomena can be attributed to the greater stiffness of the structure surrounding Point B compared to that of Point A. At the Point B location, multiple bulkheads are designated for fuel storage, and the distance from Point B to the bottom is shorter compared to that of Point A to the bottom. The reduction in structural stiffness results in an increase in the observed vibration amplitude and excitation frequency. A less rigid plate area enhances the probability of experiencing larger deflections.

IV. Conclusion

The procedure for directly measuring vibration in the POLBENG research vessel's structure, which experiences loads from the main engine, has been demonstrated through this research. The entire process was carried out in a deliberate and planned manner. The instances were given their names based on the measurements that were taken in two distinct locations, which were designated as Measurement 1 and Measurement 2. In both instances, the same treatment was administered, which consisted of the ship's main engine operating at an RPM of approximately 4,000. The peak frequency values in Measurement 2 are 5.37% lower than those in Measurement 1, recorded at 31.52 Hz and 33.31 Hz, respectively. This indicates that the oscillatory motion that occurs at the measurement point of Measurement 1 oscillates more than that which occurs

at Measurement 2. Measurement 1 has RMS values of vibration velocity that are 0.020 mm/s, while Measurement 2 has RMS values of 0.013 mm/s. This indicates that the magnitude of the response is also greater in Measurement 1 compared to Measurement 2. The explanation for the occurrence of both phenomena is due to the fact that the structure surrounding the location of Measurement 2 is more rigid than the structure surrounding Measurement 1. After everything has been assessed, the HDPE structure that was constructed is able to endure the vibrations that are generated by the ship's main engine operations. When compared to the value that is standardized by the class, the RMS values at both measurement locations do not exceed the value. On the other hand, the values of the peak frequencies of both do not coincide with the values of the natural frequencies.

ACKNOWLEDGEMENTS

We would like to express our gratitude to Polytechnic of Bengkalis for their generous support in financing this research through the PNBP research scheme, namely Penelitian Penugasan with the contract number of 107/KT-PN/P3M-PB/2025. We would like to express our sincere gratitude for the support and resources offered by the Department of Naval Architecture, Polytechnic of Bengkalis, which have been instrumental in the successful completion of this research.

REFERENCES

[1] N. N. Alias, I. Y. A. Fatah, Y. B. Seok, S. H. Y. S. Abdullah, A. H. Bhat, and S. B. M. Diah, 'Material Characterizations of the Polymers Reinforced with Recycled Flexible Plastic Blends as Filament for 3D Printing', *ARASET*, vol. 37, no. 1, pp. 1–15, Jan. 2024, doi: 10.37934/araset.37.1.115.

[2] Siswandi B. and W. D. Aryawan, 'High Density Polyethylene (HDPE) Vessel of Pompong as a Fishing Vessel for Bengkalis Fisherman', *IJPS*, vol. 2, no. 1, pp. 108–113, May 2017, doi: 10.12962/j23546026.y2017i2.2306.

[3] D. Setiawan, A. Sulisetyono, W. D. Aryawan, and R. C. Ariesta, 'Experimental Study on Fracture Toughness of HDPE Material with Compact Tension Specimens for Small Vessel', *JARASET*, vol. 57, no. 3, pp. 35–45, Oct. 2024, doi: https://doi.org/10.37934/araset.57.3.3545.

[4] D. Dallé, L. V. Rossa Beltrami, C. Borsoi, and A. J. Zattera, 'Effect of different nanofillers incorporation on HDPE/LDPE films nanocomposite', *Journal of Reinforced Plastics and Composites*, p. 07316844241239253, Mar. 2024, doi: 10.1177/07316844241239253.

[5] J. Wang, M. Gahleitner, F. Berger, and K. Bernreitner, 'Polymer Composition Suitable for Making Films', EP4067432B1, Nov. 15, 2023 [Online]. Available: https://iopscience.iop.org/article/10.1088/1742-6596/2907/1/012015/pdf

[6] A. Koriem, A. M. Ollick, and M. Elhadary, 'The effect of artificial weathering and hardening on mechanical properties of HDPE with and without UV stabilizers', *Alexandria Engineering Journal*, vol. 60, no. 4, pp. 4167–4175, Aug. 2021, doi: 10.1016/j.aej.2021.03.024.

[7] A. K. Sahu and K. Sudhakar, 'Effect of UV exposure on bimodal HDPE floats for floating solar application', *Journal of Materials Research and Technology*, vol. 8, no. 1, pp. 147–156, Jan. 2019, doi: 10.1016/j.jmrt.2017.10.002.

[8] P. Wibawa *et al.*, 'Analysis of tensile and flexural strength of HDPE material joints in ship construction', *J Appl Eng Science*, vol. 21, no. 2, pp. 668–677, 2023, doi: 10.5937/jaes0-41924.

[9] L. F. Kadhim, 'Mechanical Properties of High Density Polyethylene/Chromium Trioxide under Ultraviolet Rays', vol. 12, no. 10, 2017.

[10] G. Santos, E. Esmizadeh, and M. Riahinezhad, 'Recycling Construction, Renovation, and Demolition Plastic Waste: Review of the Status Quo, Challenges and Opportunities', *J Polym Environ*, vol. 32, no. 2, pp. 479–509, Feb. 2024, doi: 10.1007/s10924-023-02982-z.

[11] M. Kafalı, 'A Research on Design and Production of HDPE Boat Structural Elements', in *International Naval Architecture and Maritime Symposium*, Istanbul: The 4th International Naval Architecture and Maritime Symposium (INT-NAM 2023), Nov. 2023, pp. 683–691.

[12] A. Sözen and G. Neşer, 'High Density Polyethylene (HDPE) as a Prominent Marine Small Craft Building Material: Opportunities and Obstacles.', in *The 25th Symposium on Theory and Practice of Shipbuilding*, Malinska: BRODOGRADNJA, 2022, pp. 89–90.

[13] R. V. Patel, A. Yadav, and J. Winczek, 'Physical, Mechanical, and Thermal Properties of Natural Fiber-Reinforced Epoxy Composites for Construction and Automotive Applications', *Applied Sciences*, vol. 13, no. 8, p. 5126, Apr. 2023, doi: 10.3390/app13085126.

[14] S. Huang *et al.*, 'Plastic Waste Management Strategies and Their Environmental Aspects: A Scientometric Analysis and Comprehensive Review', *IJERPH*, vol. 19, no. 8, p. 4556, Apr. 2022, doi: 10.3390/ijerph19084556.

[15] P. A. Popescu, E. E. Popa, A. C. Mitelut, and M. E. Popa, 'Development of Recyclable and Biodegradable Food Packaging Materials – Opportunities and Risks', *CTNS*, vol. 9, no. 17, pp. 142–146, Jul. 2020, doi: 10.47068/ctns.2020.v9i17.016.

[16] D. Setyawan, A. Sulisetyono, and W. Aryawan, 'Effect of additional grip on tensile strength of non-ferrous materials for ship', *J Appl Eng Science*, vol. 20, no. 4, pp. 1175–1183, 2022, doi: 10.5937/jaes0-37093.

[17] M. Zulbakri *et al.*, 'Experimental Investigations on Mechanical Properties of Virgin and Recycled High-Density Polyethylene (HDPE) for the Blown Film Extrusion', *J. Phys.: Conf. Ser.*, vol. 2907, no. 1, p. 012015, Dec. 2024, doi: 10.1088/1742-6596/2907/1/012015.

[18] M. M. Hashim, N. Marsi, T. Letchumanan, A. Z. Mohd Rus, M. R. Mohd Jamir, and N. Hassan, 'Bending strength analysis of HDPE plastic reinforced wood waste and thermoplastic polymer to replace ceramic tile composites', *J. Phys.: Conf. Ser.*, vol. 2051, no. 1, p. 012045, Oct. 2021, doi: 10.1088/1742-6596/2051/1/012045.

[19] W. Elhrari, 'The Influence of LDPE Content on the Mechanical Properties of HDPE/LDPE Blends', *RDMS*, vol. 7, no. 5, Aug. 2018, doi: 10.31031/RDMS.2018.07.000672.

[20] B. Moon, H. Hong, D.-H. Kim, W. Lee, and S. Lee, 'Comparative Study on Load Criteria by Class Based on Structural Analysis of 38ft HDPE Power Boat', *SNAK*, vol. 60, no. 1, pp. 38–47, Feb. 2023, doi: 10.3744/SNAK.2023.60.1.38.

[21] J.-M. Lee, 'Feasibility study of shell element-based elastic FE approach for welding-induced thermal distortion prediction in HDPE welded structures', *International Journal of Naval Architecture and Ocean Engineering*, vol. 15, p. 100559, 2023, doi: 10.1016/j.ijnaoe.2023.100559.

[22] W. S. Vorus, 'Vibration', in *Principle of Naval Architecture (Second Revision)*, vol. Resistance, Propulsion, and Vibration, II vols, Jersey City, NJ: The Society of Naval Architects and Marine Engineers, 1988, pp. 255–316.

[23] ABS, *Guidance Notes on Ship Vibration*, Ship Vibration. Spring: American Bureau of Shipping, 2023.

[24] W. T. Thomson, *Theory of Vibration with Aplications*, Fourth Edition. California: Taylor & Francis, 2010.

[25] ISSC, 'Damage Assessment After Accidental Events'. International Ship and Offshore Structures Congress, Aug. 2009. Accessed: May 14, 2025. [Online]. Available: http://www.issc2025.com/Public/uploads/DAMAGE-ASSESSMENT-AFTER-ACCIDENTAL-EVENTS.pdf

[26] Z. Zhang, K. Shankar, E. V. Morozov, and M. Tahtali, 'Vibration-based delamination detection in composite beams through frequency changes', *Journal of Vibration and Control*, vol. 22, no. 2, pp. 496–512, Feb. 2016, doi: 10.1177/1077546314533584.

[27] C. Yang, X. Hou, L. Wang, and X. Zhang, 'Applications of different criteria in structural damage identification based on

natural frequency and static displacement', *Sci. China Technol. Sci.*, vol. 59, no. 11, pp. 1746–1758, Nov. 2016, doi: 10.1007/s11431-016-6053-y.

[28] M. Carminati and S. Ricci, 'Structural Damage Detection Using Nonlinear Vibrations', *International Journal of Aerospace Engineering*, vol. 2018, pp. 1–21, Sep. 2018, doi: 10.1155/2018/1901362.

[29] A. A. Shabana, *Theory of Vibration: An Introduction*, Third Edition., vol. An Introduction. in Mechanical Engineering Series, vol. An Introduction. Chicago: Springer International Publishing, 2019. doi: 10.1007/978-3-319-94271-1.

[30] I. A. Karnovsky and E. Lebed, *Theory of Vibration Protection*. Coquitlam: Springer International Publishing, 2016. doi: 10.1007/978-3-319-28020-2.

[31] K. Hinkelmann, O. Kempthorne, and K. Hinkelmann, Eds., *Design and analysis of experiments*, Second Edition., 1 vols. in Wiley series in probability and statistics. Hoboken, N.J: Wiley-Interscience, 2008.

[32] Y. Wang, M. Gao, H. Ouyang, S. Li, Q. He, and P. Wang, 'Modelling, simulation, and experimental verification of a pendulum-flywheel vibrational energy harvester', *Smart Mater. Struct.*, vol. 29, no. 11, p. 115023, Nov. 2020, doi: 10.1088/1361-665X/abacaf.

[33] S. Usman and Muh. Anhar, 'Condition Monitoring for Induction Motor using Wireless Vibration Monitoring System', in *Proceedings of the International Conference on Applied Science and Technology on Engineering Science 2023 (iCAST-ES 2023)*, M. U. H. Al Rasyid and M. R. Mufid, Eds., in Advances in Engineering Research, vol. 230. Dordrecht: Atlantis Press International BV, 2024, pp. 1151–1162. doi: 10.2991/978-94-6463-364-1_105.

[34] C. V. Amaechi, F. Wang, and J. Ye, 'Experimental Study on Motion Characterisation of CALM Buoy Hose System under Water Waves', *JMSE*, vol. 10, no. 2, p. 204, Feb. 2022, doi: 10.3390/jmse10020204.

[35] C. V. Amaechi, F. Wang, and J. Ye, 'Numerical Assessment on the Dynamic Behaviour of Submarine Hoses Attached to CALM Buoy Configured as Lazy-S under Water Waves', *JMSE*, vol. 9, no. 10, p. 1130, Oct. 2021, doi: 10.3390/jmse9101130.

[36] M. Määttänen, P. Marjavaara, and S. Saarinen, 'Ice Crushing Pressure Distribution Against a Compliant Stiffened Panel', in *Proceedings of the 21st International Conference on Port and Ocean Engineering under Arctic Conditions*, in 38, vol. 21. Montréal: Port and Ocean Engineering under Arctic Conditions (POAC), Jul. 2011. [Online]. Available: http://www.poac.com/PapersOnline.html

[37] T. Takeuchi, M. Sakai, S. Akagawa, N. Nakazawa, and H. Saeki, 'On the Factors Influencing the Scaling of Ice Forces', in *IUTAM Symposium on Scaling Laws in Ice Mechanics and Ice Dynamics*, J. P. Dempsey and H. H. Shen, Eds., in Solid Mechanics and Its Applications, vol. 94. Dordrecht: Springer Netherlands, 2001, pp. 149–160. doi: 10.1007/978-94-015-9735-7_13.

[38] H. Hendrikse and A. Metrikine, 'Interpretation and prediction of ice induced vibrations based on contact area variation', *International Journal of Solids and Structures*, vol. 75–76, pp. 336–348, Dec. 2015, doi: 10.1016/j.ijsolstr.2015.08.023.

[39] P. Su, J. Wu, and S. Liu, 'Analysis and Experimental Research on Vibration Characteristics of Pressure Shell Structure', *Exp Tech*, vol. 48, no. 1, pp. 3–13, Feb. 2024, doi: 10.1007/s40799-023-00638-0.

[40] J. A. Gallego-Juarez, *Power Ultrasonics: Applications of High-Intensity Ultrasound*, 2nd ed. in Woodhead Publishing Series in Electronic and Optical Materials Series. San Diego: Elsevier Science & Technology, 2023.

[41] D. H. Nguyen, T. T. Bui, G. D. Roeck, and M. A. Wahab, 'Damage detection in Ca-Non Bridge using transmissibility and artificial neural networks', *Structural Engineering and Mechanics*, vol. 71, no. 2, pp. 175–183, 2019, doi: 10.12989/SEM.2019.71.2.175.

[42] J. Xu, M. Hong, and X. Liu, 'Operational modal analysis of a ship model in the presence of harmonic excitation', *J. Marine. Sci. Appl.*, vol. 12, no. 1, pp. 38–44, Mar. 2013, doi: 10.1007/s11804-013-1167-8.

[43] R. B. Hageman and I. Drummen, 'Modal analysis for the global flexural response of ships', *Marine Structures*, vol. 63, pp. 318–332, Jan. 2019, doi: 10.1016/j.marstruc.2018.09.012.

[44] T. Pais and P. Silvestri, 'Full scale cruise ship dynamic identification using operational modal analysis on sea trial data measurements', *Ocean Engineering*, vol. 311, p. 118931, Nov. 2024, doi: 10.1016/j.oceaneng.2024.118931.

[45] A. Metcalfe, L. Maurits, T. Svenson, R. Thach, and G. E. Hearn, 'Modal analysis of a small ship sea keeping trial', *ANZIAMJ*, vol. 48, p. 915, Jul. 2007, doi: 10.21914/anziamj.v47i0.1082.

[46] S. Krishnan, *Biomedical signal analysis for connected healthcare*. London: Academic Press, 2021.

[47] Y. Zhao, S. Huang, X. Wang, J. Shi, and S. Yao, 'Energy management with adaptive moving average filter and deep deterministic policy gradient reinforcement learning for fuel cell hybrid electric vehicles', *Energy*, vol. 312, p. 133395, Dec. 2024, doi: 10.1016/j.energy.2024.133395.

[48] H. Mengzhuo, G. Cong, and C. Hui, 'Energy Management Strategy of Fuel Cell Ship Based on Moving Average Transformation', in *2023 IEEE International Conference on Electrical, Automation and Computer Engineering (ICEACE)*, Changchun, China: IEEE, Dec. 2023, pp. 1–6. doi: 10.1109/iceace60673.2023.10442221.

[49] J. Park, J. Kim, and N. Son, 'Passive target tracking of marine traffic ships using onboard monocular camera for unmanned surface vessel', *Electronics Letters*, vol. 51, no. 13, pp. 987–989, Jun. 2015, doi: 10.1049/el.2015.1163.

[50] T. Pereira, V. Santos, T. Gameiro, C. Viegas, and N. Ferreira, 'Evaluation of Different Filtering Methods Devoted to Magnetometer Data Denoising', *Electronics*, vol. 13, no. 11, p. 2006, May 2024, doi: 10.3390/electronics13112006.

[51] J. Sha, M. Fan, B. Cao, and B. Liu, 'Noncontact and nondestructive evaluation of heat-treated bearing rings using pulsed eddy current testing', *Journal of Magnetism and Magnetic Materials*, vol. 521, p. 167516, Mar. 2021, doi: 10.1016/j.jmmm.2020.167516.

[52] N. K. Mutlib, M. N. Ismael, and S. Baharom, 'Damage Detection in CFST Column by Simulation of Ultrasonic Waves Using STFT-Based Spectrogram and Welch Power Spectral Density Estimate', *Structural Durability & Health Monitoring*, vol. 15, no. 3, pp. 227–246, 2021, doi: 10.32604/sdhm.2021.010725.

[53] G. B. Rossi, F. Crenna, V. Piscopo, and A. Scamardella, 'Comparison of Spectrum Estimation Methods for the Accurate Evaluation of Sea State Parameters "2279', 2020.

[54] P. Welch, 'The use of fast Fourier transform for the estimation of power spectra: A method based on time averaging over short, modified periodograms', *IEEE Trans. Audio Electroacoust.*, vol. 15, no. 2, pp. 70–73, Jun. 1967, doi: 10.1109/TAU.1967.1161901.

[55] K. J. Vamvoudakis-Stefanou, J. S. Sakellariou, and S. D. Fassois, 'Output-Only Statistical Time Series Methods for Structural Health Monitoring: A Comparative Study', 2014.

[56] H. Fang, Y. Ji, S. Li, H. Liu, and D. Wang, 'RHES: Development of real-time health evaluation system based on human pulse signal utilizing PVDF/PDMS arch-type piezoelectric sensor', *Measurement*, vol. 224, p. 113856, Jan. 2024, doi: 10.1016/j.measurement.2023.113856.

[57] M. I. Hatamleh, J. Mahadevan, A. Malik, and D. Qian, 'Variable Damping Profiles Using Modal Analysis for Laser Shock Peening Simulation', *Journal of Manufacturing Science and Engineering*, vol. 140, no. 5, p. 051006, May 2018, doi: 10.1115/1.4039196.

[58] R. Ballesteros-Tajadura, S. Velarde-Suárez, and J. P. Hurtado-Cruz, 'Noise Prediction of a Centrifugal Fan: Numerical Results and Experimental Validation', *Journal of Fluids Engineering*, vol. 130, no. 9, p. 091102, Sep. 2008, doi: 10.1115/1.2953229.

[59] W. Neise, 'Noise reduction in centrifugal fans: A literature survey', *Journal of Sound and Vibration*, vol. 45, no. 3, pp. 375–403, Apr. 1976, doi: 10.1016/0022-460X(76)90394-1.

[60] W. Neise, 'Review of Noise Reduction Methods for Centrifugal Fans', *Journal of Engineering for Industry*, vol. 104, no. 2, pp. 151–161, May 1982, doi: 10.1115/1.3185810.

[61] J.-C. Cai, D.-T. Qi, and Y.-H. Zhang, 'A Numerical Study of the Blade Passing Frequency Noise of a Centrifugal Fan', in *Volume 12: Vibration, Acoustics and Wave Propagation*, Houston, Texas, USA: American Society of Mechanical Engineers, Nov. 2012, pp. 335–343. doi: 10.1115/IMECE2012-86745.

[62] L. You, W. Fan, Z. Li, Y. Liang, M. Fang, and J. Wang, 'A Fault Diagnosis Model for Rotating Machinery Using VWC and MSFLA-SVM Based on Vibration Signal Analysis', *Shock and Vibration*, vol. 2019, no. 1, p. 1908485, Jan. 2019, doi: 10.1155/2019/1908485.

[63] D. Klimenko, A. Kondratov, S. Timushev, and J. Li, 'Study of BPF pressure pulsations reduction in centrifugal bladed machines using splitters', *J. Phys.: Conf. Ser.*, vol. 1925, no. 1, p. 012063, May 2021, doi: 10.1088/1742-6596/1925/1/012063.

[64] Y. Park, M. Jeong, S. B. Lee, J. A. Antonino-Daviu, and M. Teska, 'Influence of Blade Pass Frequency Vibrations on MCSA-Based Rotor Fault Detection of Induction Motors', *IEEE Trans. on Ind. Applicat.*, vol. 53, no. 3, pp. 2049–2058, May 2017, doi: 10.1109/TIA.2017.2672526.

[65] S. Shi, W. Tang, X. Huang, X. Dong, and H. Hua, 'Experimental and numerical investigations on the flow-induced vibration and acoustic radiation of a pump-jet propulsor model in a water tunnel', *Ocean Engineering*, vol. 258, p. 111736, Aug. 2022, doi: 10.1016/j.oceaneng.2022.111736.

[66] A. Youssef, 'Investigation Into the Vibration Properties of Marine Propulsion Systems', Dissertation, The University of Western Australia, Crawley, 2019.

[67] W. Zhang, F. Li, J. Ma, X. Ning, S. Sun, and Y. Hu, 'Fluid-structure interaction analysis of the rudder vibrations in propeller wake', *Ocean Engineering*, vol. 265, p. 112673, Dec. 2022, doi: 10.1016/j.oceaneng.2022.112673.

[68] L. Hasse, 'Basic Atmospheric Structure And Concepts: Beaufort Wind Scale', in *Encyclopedia of Atmospheric Sciences*, Elsevier, 2015, pp. 1–6. doi: 10.1016/B978-0-12-382225-3.00466-7.